



# Using Elastic Properties as a Predictive Tool to Identify Pore-Fluid Type in Carbonate Formations

Mahmoud Jasim Al-Khafaji and Wafaa' Mustafa Al-Kattan

*Petroleum Engineering Department-College of engineering- University of Baghdad*

## Abstract

The aim of this study is for testing the applicability of Ramamoorthy and Murphy method for identification of predominant pore fluid type, in Middle Eastern carbonate reservoir, by analyzing the dynamic elastic properties derived from the sonic log, and involving the results of Souder, for testing the same method in chalk reservoir in the North Sea region. Mishrif formation in Garraf oilfield in southern Iraq was handled in this study, utilizing a slightly-deviated well data, these data include open-hole full-set logs, where, the sonic log composed of shear and compression modes, and geologic description to check the results. The Geolog software is used to make the conventional interpretation of porosity, lithology, and saturation. Also, include PVT and water analyses as inputs in Batzle and Wang correlations in order to calculate mechanical properties of oil and water at reservoir conditions. The shear velocity and density logs are used to calculate the shear modulus (G), for each (0.1254) meter. The dry frame bulk modulus correlation of the original method was not followed, instead, a new dry frame bulk modulus correlation of Saxena is used to avoid the uncertainty in the porosity type exist in the formation which needs special core description. Then, Gassmann's equations were used to determine the bulk moduli of the rock assuming two saturation conditions; the first is 100% water saturated, and the second is 100% oil saturated. Using elastic properties equations of Love's, and the resulted bulk moduli, two corresponding  $\Delta t(s)$ , (for oil and for water), were computed for each depth level. Then these  $\Delta t(s)$  were plotted with sonic  $\Delta t$  in the same track, and compiled with the conventional log interpretation, to compare the results. The method was a good indicator of the fluid type in the high porosity zones, unlike for the tight or clay-rich zones. The results are very conformable to the conventional interpretation, the OWC in both model and conventional interpretation are so close with error percentage of (0.03%).

*Keywords: Elastic Properties, Mishrif Formation, sonic log.*

*Received on 10/10/2018, Accepted on 18/12/2018, published on 30/03/2019*

<https://doi.org/10.31699/IJCPE.2019.1.8>

## 1- Introduction

Fluid identification from well logs depends on the radioactive logs (neutron and density) and resistivity, which do not always give the true fluid type in the formation especially in the shaly and low resistivity. Hence, the need for a new method independent from resistivity and neutron/density method and more accurate is required.

The sonic log applications in petrophysics, witnessed an obvious advancement, recently.

Where, researches presented many of its great advantages, as an interpretive tool in petrophysics.

This study described the application of a method published by Ramamoorthy and Murphy [1], to identify the dominated pore fluid type in a high porosity Middle-Eastern carbonate using modern logs and the work of Souder [2], who used a similar principle to predict pore fluid type in chalk reservoir in the North Sea.

### 1.1. The Physics of Sonic Log

The monopole transmitter in the sonic tool emits sonic waves, which, also known as “Elastic waves”, who are mechanical disturbances that propagate through the formation rocks. Such waves are able to travel over very long distances through the formation, and thus bring us information about portions of the formation that are otherwise inaccessible [3].

These waves in rocks propagate with a velocity that is given by elastic properties and the density of the rock [4].

These parameters depend on other parameters such as porosity, pressure, mineral composition, depth, and fluid type and saturation [5].

Thus elastic waves also provide a method by which specific formation parameters can be estimated in the field.

These elastic waves that propagate in a fluid-filled borehole into the formation during sonic logging operation are known as body waves, where two important types of energy transport mechanisms are supported by the elastic media (formation): compressional waves and shear waves.

Where, the compressional waves, also known as Longitudinal Waves, in this wave the particles move in a direction parallel to the direction of propagation.

The speed of propagation is largest for this kind of wave compared to others and so it arrives first. It is the only wave propagated in liquids [6].

While the shear waves, also known as Transverse Waves, Particle movement is in a direction perpendicular to the wave direction.

As mentioned, the speed of propagation is less than the P-wave with a ratio of about (1.6–2). No shear waves are transmitted in fluids because the presence of shear waves requires the medium to possess shear strength. In the formation, sound energy is transmitted by both compressional and shears waves. In the mud, energy is transmitted solely by compressional waves.

The energy transmitted by the slower shear wave is much higher than that of the compressional wave which is first to arrive. In the wave pattern received, we can identify the shear wave by this feature [6], see Fig. 1.

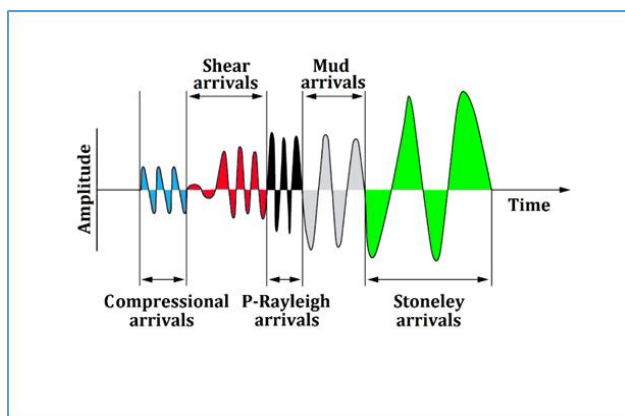


Fig. 1. Time vs Amplitude plot illustrating sonic wave's arrival sequence, Ref [4]

## 1.2. Study Objectives

In this study, the applicability of a method using sonic waves as a qualitative tool, to identify the presence of hydrocarbon as a prevailed pore fluid in Mishrif formation in southern Iraq, was tested, by applying the result of work of Ramamoorthy and Murphy [1], to identify the dominated pore fluid type in a high porosity Middle-Eastern carbonate using modern logs and the work of Souder [2], who used a similar principle to predict pore fluid type in chalk reservoir in the North Sea.

## 2- Area of Case Study and Geologic Setting

Mishrif Formation which is a carbonate formation of Cretaceous age was deposited in Mesopotamian Basin during the late Cenomanian to Early Turonian (95 MA) [7].

Mishrif formation is handled in this study in Garraf oilfield within the Euphrates subzone in the Mesopotamian zone of the stable shelf [8], Fig. 2, Garraf oilfield is situated in southern Iraq, in Thi Qar Governorate about 85km to the north of Nassriya city, Fig. 2.

This oilfield was discovered in 1984. It has low relief gentle anticlinal structure aligned in NW-SE direction and has a dimension of (10km in width x 31 km in length) [9].

It has proven by exploration and appraisals wells in Garraf, to have hydrocarbon accumulation in primary oil accumulation zones, which are the Mishrif and Yamama Formations, Mishrif contains 70% of the field's reserve [9], and secondary accumulation zones, are in Ratawi and Zubair Formations, as shown in (Appendix A).

## 3- Shear and Bulk Moduli

### 3.1. Bulk modulus (K)

Also known as "*incompressibility*", it is a measure of the stress/strain ratio when a body is subjected to uniform compressive stress. Where, it is equal to the change in applied pressure ( $\partial P$ ) divided by the ratio of the change in volume to the original volume of a body ( $\partial V/V$ ) by [5]:

$$K = \frac{P}{\Delta V/V} \quad (1)$$

The bulk modulus is the reciprocal of the compressibility. It reflects how resistive (incompressible) is the material to an overall gain or loss of volume in conditions of hydrostatic stress.

### 3.2. Shear modulus (G)

Also known as "*modulus of rigidity*", it describes the ratio of shear stress (F/A) to shear strain ( $\theta$ ). G is defined as [5]:

$$G = \frac{F/A}{\theta} \quad (2)$$

The shear modulus is associated with a change in shape of the body where it is a measure of the ability of a solid material to resist the deformations in its shape by shear forces.

It is one of the Lamé constants. In the other hand, Fluids do not have any shear resistance, consequently zero shear modulus. So it would equal in both dry and saturation conditions for the same rock [2], [3].

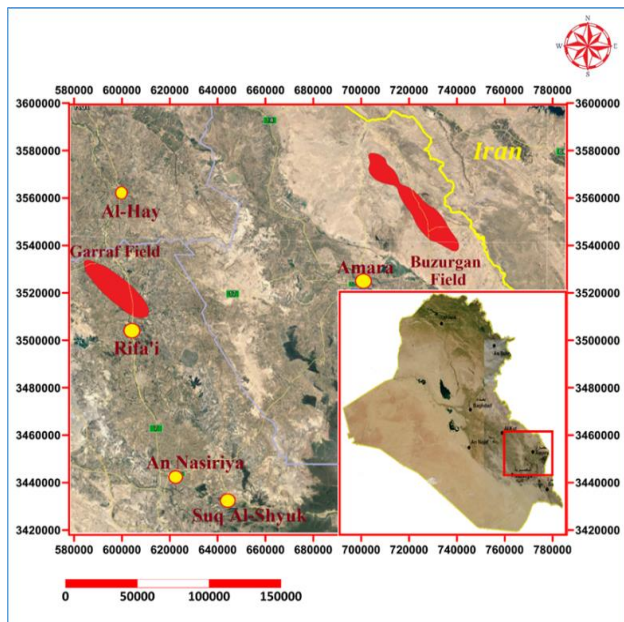


Fig. 2. Geographical Location of Area of study

4- Sonic Waves in Fluid-Saturated Porous Media

The rock-fluid system is so complicated that virtually all the theories for such a system have to make major assumptions to simplify the mathematics [10]. In order to describe the rock theoretically, it's a heterogeneous system with internal structure, which must be idealized in order to derive the formulations of elastic rock properties in terms of volume fractions and properties of the components (minerals and fluids), the rock texture, pressure, etc. In all cases, models are an idealization [11], [12]. One of the common "Models", that handle the theories of elastic properties and sonic wave's propagation in porous media, is "Gassmann Model (1951)" [13].

He developed a model for porous rocks that allows the prediction of changes in seismic velocities because of different fluid saturations in reservoirs. Where this model enables analysts to use elastic velocities in rocks saturated with one fluid to predict those of rocks saturated with a second fluid, or equivalently, predicting saturated-rock velocities from dry-rock velocities, and vice versa [11].

This is the fluid substitution problem [14]. This model relates the saturated bulk modulus of the rock to its porosity, the bulk modulus of the porous rock frame, the bulk modulus of the mineral matrix, and the bulk modulus of the pore-filling fluids, as in Eq. (3). Also, this model made the first attempt to formulate a theoretical expression for acoustic velocities in fluid-saturated porous media [15]. Gassmann's assumptions were; The porous material is isotropic, elastic, monomineralic (composed of single mineral, e.g. Calcite), and homogeneous, and Pore space is well connected and in pressure equilibrium (zero frequency limit), the medium is a closed system with no pore fluid movement across boundaries Also there is no chemical interaction between fluids and rock frame (shear modulus remains constant) [16], [13]. Gassmann model (1951), notation can be summarized, as shown in Fig. 3:

$$K_b = K_{fr} + \frac{\left(1 - \frac{K_{fr}}{K_{ma}}\right)^2}{\left(\frac{\phi}{K_{fl}}\right) + \left(\frac{1-\phi}{K_{ma}}\right) - \left(\frac{K_{fr}}{K_{ma}^2}\right)} \tag{3}$$

Where the subscripts "b", "ma", "fl", and "fr" refer to the bulk, matrix, fluid, and dry rock frame (skeleton), respectively. Note that dry-rock properties  $G_{fr}$  and  $K_{fr}$  are functions of  $\phi$ .

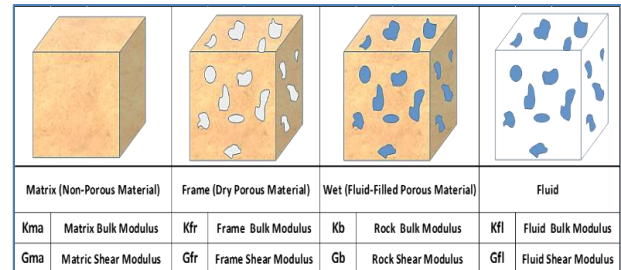


Fig. 3. Gassmann Model Notation

The major simplification incorporated is that the relative motion between the fluid and skeleton during acoustic wave propagation is negligible. The model used the bulk modulus because as mentioned above, it's more sensitive to fluid saturation, unlike the shear modulus. Therefore, any fluid saturation effect should correlate mainly to a change in the bulk modulus [16].

5- The Theory

Ramamoorthy and Murphy theory [1], on which this study has been based on, relies mainly on the shear and bulk moduli of formation, which can be computed from the relations derived by Love, Eq (4) & (5), where Love has related shear and compression wave velocities,  $V_p$  and  $V_s$  to the Elastic properties of solids through [17]:

$$G = \rho_b V_s^2 \tag{4}$$

$$K_b = \rho_b (V_p^2 - \frac{4}{3}V_s^2) \tag{5}$$

The principle of this method is that at any given depth, the porosity ( $\phi$ ), matrix bulk modulus ( $K_{ma}$ ), and frame bulk modulus ( $K_{fr}$ ), will be constant and only the bulk modulus ( $K_b$ ) will change due to change in fluid content. Thus A synthetic compressional transit time for each fluid will be calculated from the bulk modulus ( $K_b$ ), and the pore fluid is qualitatively identified by the position of the actual compressional transit time log relative to the computed curves [1], [2], [3], [5], [13].

6- Application

To apply this method, follow simple steps, which are summarized below, can be followed to compute all the necessary parameters.

- 1- perform the Pre-interpretation calculations which are:
  - from RHOB and NPHI logs, compute total porosity.

As follows:

$$\phi_T = \frac{\phi_{RHOB} + \phi_{NPHI}}{2} \tag{6}$$

- From Temperature, salinity, API, and fresh water density calculate the fluid bulk moduli and velocities of fluids (oil and water), using Batzle and Wang formulas [18], [19].

• For oil

$$\rho_{oil} = 1 \left( \frac{gm}{cm^3} \right) \times \left( \frac{141.5}{API+131.5} \right) \quad (7)$$

We consider the effect of reservoir pressure first by:

$$\rho_P = \rho_{oil} + (0.00277P - 1.71 \times 10^{-7}P^3)(\rho_o - 1.15)^2 + 3.49 \times 10^{-4} \times P \quad (8)$$

Where:

$\rho_P$ : oil density corrected for the reservoir pressure effect to account for the effect of temperature, which is larger than pressure effect:

$$\rho_{oil @ P \& T} = \frac{\rho_{@P}}{(0.972 + 3.81 \times 10^{-4}(T + 17.78))^{1.175}} \quad (9)$$

Where:

$\rho_{@P \& T}$ : oil density corrected for pressure and temperature effects, then oil density should be corrected for dissolved gas effect by involving the gas oil ratio ( $R_G$ ), which in turns depends on formation volume factor ( $B_o$ ) [19]:

$$\rho'_o = \frac{\rho_o}{B_o} (1 + 0.001R_G)^{-1} \quad (10)$$

$$R_G = 0.02123 * \gamma_{gas} \left[ P e^{\left( \frac{0.072}{\rho'_o} - 0.00377T \right)} \right]^{1.205} \quad (11)$$

$B_o$  from standings 1962 [19]:

$$B_o = 0.972 + 0.00038 \left[ 2.4R_G \left( \frac{G}{\rho'_o} \right)^{0.5} + T + 17.8 \right]^{1.175} \quad (12)$$

Using the corrected oil density for pressure, temperature, and gas effect ( $\rho'_{oil}$ ), the sonic velocity in oil will be:

$$V_{oil} = 2096 \left( \frac{\rho'_{oil}}{2.6 - \rho'_{oil}} \right)^{\frac{1}{2}} - 3.7T + 4.64P + 0.0115(4.12(1.08\rho'_o)^{-1} - 1)^{0.5} - 1)TP \quad (13)$$

For water

First, we find the fresh water density ( $\rho_w$ ) at reservoir pressure and temperature by:

$$\rho_w = 1 + 1 \times 10^{-6}(-80T - 3.3T^2 + 0.00175T^2 + 489P - 2TP + 0.016T^2P - 1.3 \times 10^{-5}T^3P - 0.333P^2) \quad (14)$$

Then using fresh water density, formation water salinity, pressure, and temperature, the Brine (formation water) density, can be calculated as:

$$\rho_{Brine} = \rho_w + S\{0.668 + 0.44S + 1 \times 10^{-6}[300P - 2400PS + T(80 + 3T - 3300S - 13P + 47PS)]\} \quad (15)$$

Then the sonic velocity in brine ( $V_{Brine}$ ) can be found from Eq (16), as:

$$V_{Brine} = V_w + S(1170 - 9.6T + 0.055T^2 - 8.5 \times 10^{-5} - 5T^3 + 2.6P - 0.0029TP - 0.0476P^2) + S^{1.5}(780 - 10P + 0.16P^2) - 820 S^2 \quad (16)$$

Where:

$V_w$ : sonic velocity in fresh water at reservoir pressure and temperature:

$$V_w = \sum_{i=0}^4 \sum_{j=0}^3 w_{ij} T^i P^j \quad (17)$$

Where:  $i/j$  as shown in Table 1.

Table 1.  $i/j$  values for Eq (17)

$i/j$	0	1	2	3
0	1402.85	1.524	3.44e-03	-0.00001197
1	4.871	-0.0111	1.74e-04	-1.63e-06
2	-0.04783	2.75e-04	-0.000002135	1.24e-08
3	1.49e-04	-6.50e-04	-1.46e-08	1.33e-10
4	-2.20e-07	7.99e-10	5.23e-11	-4.61e-13

Where:  $V_{oil}$  and  $V_{brine}$ , and  $V_w$  in m/s, API in degrees, T in Celsius Degrees, P in MPa, and S is the weight fraction (ppm/1000000) of sodium chloride. The computed properties and results of these equations are listed in Appendix B, (Tables 2&3),

1- predict fluid bulk modulus Love's expression is used, Eq (5), with ( $V_s = 0$ ) is the fluids do not sustain shear waves

2- Ramamoorthy and Murphy [1], and Souder [2],

have used lab derived quadratic correlations to derive the dry frame modulus, as in Eq (18), which are based on porosity type, and thus, detailed core analyses are needed to confirm the porosity type (either intergranular or spherical), in order to use the appropriate formula for frame bulk modulus ( $K_{fr}$ ). Where Ramamoorthy and Murphy construct these correlations from laboratory mechanical properties measurements on core samples [1], two separate trends were observed between the porosity and the ratio of the dry porous rock frame bulk modulus ( $K_{fr}$ ) to the shear modulus (G). They used scattering theory to show these trends correspond to two types of pore systems, intergranular porosity and spherical (or vugular) porosity. The graph was hand digitized and regressed in specialized statistical software to produce the best fit line, as shown in Fig. 4, they were represented by a quadratic equation of the formula [2], [5]:

$$\frac{K_{fr}}{G} = constant + a. \phi + b. \phi^2 \quad (18)$$

They Compute the Shear modulus (G) using Love Expression, Eq (4), where the inputs are expressed using the appropriate unit conversion constant, the shear wave slowness  $\Delta T_s$  in units of psi/ft., the bulk density  $\rho_b$  in gm/cc, and the shear modulus in units of Gigapascals (GPa) as:

$$G = \frac{92903 \times \rho_b}{\Delta t_s^2} \quad (19)$$

To avoid the necessity for core analyses, which are not always available, and if available sometimes not so much detailed to tell the porosity type, therefore, in this study a better representative correlation was implemented, to compute dry frame bulk modulus, which is dependent on lithology, not on porosity type.

Hence, no need to know the porosity type, which is very heterogenous in nature, where it may be different in new wells from that well where the core was taken from. And from the application it gives a very precise prediction, instead of the relations suggested by the previous authors, where their correlations led to misleading results in many occasions, in addition to that, they are of limited benefit in zones, where the porosity is less than 10 p.u.

Saxena [20], found that from laboratory data, it is possible to estimate a theoretical dry frame bulk modulus, only from lithological considerations knowing their porosity and  $V_p$  to  $V_s$  ratio. the proposed relation is combined with the advantage of Pickett's unique result of constant  $V_p/V_s$  ratio of (1.9) in limestone independent of pressure and porosity [21]. It leads to evaluate a dry frame bulk modulus from porosity in an exponential equation, of the form:

$$K_{fr} = \frac{((\frac{V_p}{V_s})^2 - \frac{4}{3})}{C} \quad (20)$$

Where

$$C = 10^{(2.3268*\Phi - 1.45578)} \quad (21)$$

$K_{fr}$ : dry frame bulk modulus, GPa.

$V_p/V_s$ : compressional to shear velocity ratio, unitless

$\Phi$ : porosity, fraction.

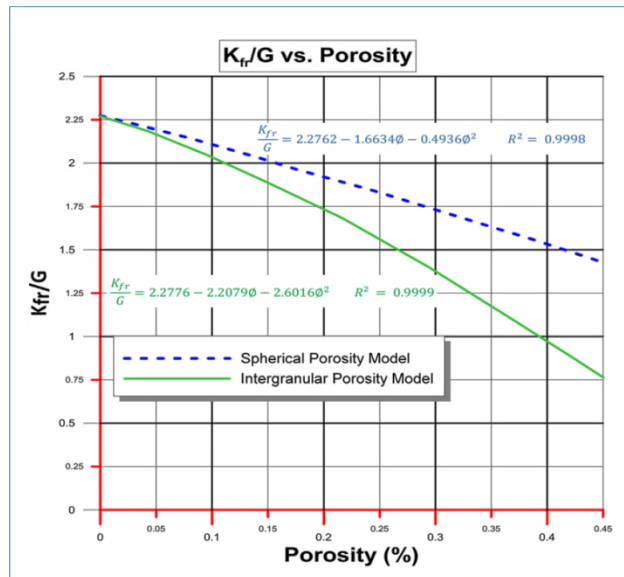


Fig. 4. Laboratory measurements of the ratio of the bulk modulus  $K_{fr}$  of a dry porous limestone ("framework") to the shear modulus of the same specimen plotted against porosity for a number of samples.

Acoustic scattering theory was used to determine that two types of pores exist in this sample set, and the lines fit these respective pore models [1]

Since the fluids commonly encountered in the borehole environment cannot support shear stresses ( $G_f=0$ ), as mentioned earlier, consequently, the shear modulus ( $G_b$ ) of a fluid-saturated porous rock will be identical to the dry porous rock shear modulus ( $G_{fr}$ ), because it related to the

solid part of the rock only, and ( $G$ ) will be used in equations for both dry and fluid-saturated rocks.

- 3- The bulk modulus of the formation  $K_b$ , then can be computed from  $K_{fr}$ , porosity, pore fluid bulk modulus  $K_f$  and the matrix bulk modulus  $K_{ma}$  using an equation of Gassmann, (Eq 3). Thus, at any particular depth,  $\phi$ ,  $K_{ma}$ , and  $K_{fr}$  are constant and the bulk modulus will change as the fluid content is altered, so a new fluid bulk modulus will be assigned to each type of fluids, (oil and water), respectively. It can be used to predict fluid type in the reservoir, and to monitor fluid in the reservoir with time.
- 4- From Love formula [17], using the two different fluid moduli corresponding to oil, and water. From each of these bulk moduli, compressional travel time can be calculated:

$$\Delta T_c = \sqrt{\frac{92903\rho_b}{K + \frac{4}{3}G}} \quad (22)$$

- 5- After the two fluid compressional wave travel times corresponding to the two different fluids have been calculated for each depth, a well log plot is generated of them and the actual logged compression wave slowness is superimposed on the same plot.
- 6- The calculated curve that best matches the measured  $\Delta T_c$  log identifies the fluid, because of the bulk modulus will be identical to the actual modulus.

## 7- Results and Discussion

Ramamoorthy and Murphy [1], showed that they have concluded a method to predict the relative amounts of spherical and intergranular porosity at each depth level, but did not divulge how this is accomplished. Since no method for making this distinction was available, Souder [2], used in his study, generated two separate sets of curves for a test well, for each of the relationships in Fig. 4 (that is, using two different sets of coefficients in Eq (14), but, as long as the core analysis is still immature in the study area, so the results could be highly erroneous, when the porosity type is unknown for sure. Hence a new correlation for dry frame bulk modulus was involved instead of the previous procedure followed by previous authors, hence Saxena's equation [19], was used, which requires only the type of lithology and if it is unknown, the velocity ratio can be used directly, even the results are much more realistic than the previous method.

Appendix (C) represents a well log plot of these result sets of model curves for the studied well in Garraf oilfield, which is targeting Mishrif reservoir and using open hole log data as input Including zone by zone comparison and discussion along the well. The well was drilled to the Mishrif reservoir as predominantly oil producing well which under-saturated oil is bearing formation.

Matrix bulk modulus used (in GPa units) is ( $K_{ma} = 70.3$ ) GPa, for limestone. While the parameters of fluids (oil and water), used in the correlations are listed in (Appendix B: Table 2 & 3), respectively. As shown in Fig. 5, that the brine bulk modulus values of Mishrif water-bearing zones are varying with small increments almost equal, due to density and velocity values are almost equal, as the Temperature, and salinity of the different Mishrif members are similar, despite the slightly increasing pressure with depth.

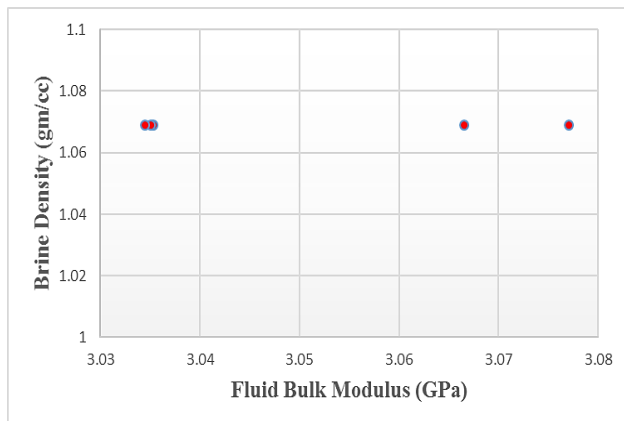


Fig. 5. Brine bulk modulus vs density of water-bearing zones of Mishrif formation

In Fig. 6, oil bulk modulus vs API gravity, where it is obvious that the bulk modulus is decreasing with increasing API gravity, which in turn is increasing with depth in our case study, due to the effect of dissolved gases is higher, where we can see the difference between the dead oil and live oil bulk modulus values in Appendix B, (table2), where the effect of gases in live oil, reduced the values of bulk modulus vitally.

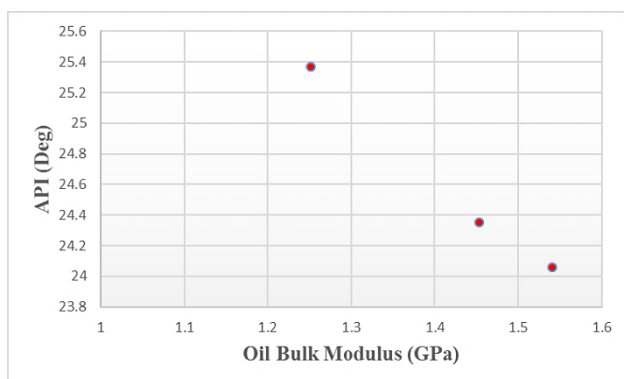


Fig. 6. Live oil bulk modulus vs API gravity of oil-bearing zones of Mishrif formation

(Appendix C), represent the conventional interpretation of open hole data and the proposed method modeled curves, the depths provided are in measured depth and TVDSS, the first track includes gamma-ray and bit size and caliper logs, the second represents the effective and total porosities (PHIE, PHIT) respectively, in addition to sonic porosity (PHI).

The fourth track contains water saturation. The fifth track represents the rock constituents (fluids, minerals, and porosity). The proposed method models are represented in the third track where it contains the three transit time curves, the black is the sonic transit time, blue is model water transit time, and the red is model oil curve.

In the top of Mishrif formation, where it called upper Mishrif U1, its top at 2268 m, it is a tight zone with porosity less than 8% p.u. the sonic travel time does not match with the model transit time curves, and the water and oil curves are overlaid, with less value. This behavior is obvious in each tight zone along the formation, where, this behavior is repeated in middle Mishrif, it can be seen in the top of M1 from 2336 to 2339, and also in M2 zone from 2352 to 2375.5 m. this behavior can be traced back to the lower value of the porosity which is involved in both dry frame and bulk rock modulus values, where it will affect these values to a great extent. For the water zone in upper Mishrif, U2 from 2295 to 2330.5, the oil model curve shows high transit time, in comparison to the sonic and model water curve, which are matched well, and gives good indication for water-bearing zone, except for 10 meters from 2302 to 2312, where the sonic tool suffered from tool malfunction and there was a problem in the data telemetry.

The match between model water curve and sonic transit time is good as long as the porosity is high, where we can see the interval from 2316 to 2318 where porosity decreases the match between curves is misleading. Because it shows an oil zone instead of water due to the match is more to oil curve than for the water one. For the Marl zone, from 2331 to 2336 m, where it composed of 40% Calcite, and 60% Clay minerals. Where the Gamma Ray curve reads an average around 100 GAPI, which is the cap-rock of the reservoir.

The curves show no match at all, due to the tool erroneous readings as the hole suffered from severe washout, as the caliper log reads 17 inches' enlargement, while the bit size is 8.5 inches that cause the sonic tool to shows abnormal readings.

For the model, the two curves of oil and water, both show abnormal behavior, due to that the density and neutron readings are highly affected by the washout, so the porosity is overestimated and wrapped more than 0.50 p.u., which is not a real case, thus it has contributed to the model as a wrong value, in addition to the sonic log abnormal values.

For the oil zones below, M1, from 2336 to 2352, is the first oil-bearing zone, it has fair reservoir characteristics, the top of M1 from 2336 to 2339 it is a tight zone of porosity less than 0.02 p.u.

The behavior of curves is similar to U1 and M2, where the two model curve show low transit time values and overlies.

From 2339 to 2352 it is fair in characteristics of water saturation around 52% average, and porosity of about 0.21 p.u. the model oil curve is well matched with the sonic transit time, while the model water shows lower values and there is a clear separation between water and oil curves, which indicates oil-bearing zone.

For L1.1 reservoir, from 2358 to 2360.8 it shows a good match between sonic transit time and model oil curve, and from 2360.8 to 2362, a tight streak shows the same behavior for other tight zones. For the main pay zone of L1.2 from 2362.5 to 2400, it shows an excellent match between sonic curve and model oil curve a very clear separation between them and that of model water curve which displays lower transit time values. And for L2 reservoir where it composed of two systems; oil from 2400 to 2412.9, where the OWC from open hole conventional interpretation is at 2412.9, and water from 2412.9 to total depth. In this zone, the oil saturation increases from 60% to 100%, which indicates it is the transition zone of the reservoir. The match is still a good and clear separation between the water and the oil curves. And the OWC from a model is at 2413.8 with an error value of 0.03%. the sudden change in curve matching from oil to water, as traced back to the model itself, as the fluid properties are involved in two separate curves, each one represents different pore fluid, and that is the reason why there is no gentle change from oil to water in the transition zone. The rest of L2 is water-bearing zone, where the sonic and model water curve are matched well.

## 8- Conclusion

- 1- The Ramamoorthy and Murphy method is a valuable non-conventional method to detect the type of pore fluid within the area of study.
- 2- The method relies on the Gassmann theory, so it follows all Gassmann theory assumptions.
- 3- The lithology type needs to be known, in order to use the appropriate solid matrix parameters.
- 4- The dry frame bulk modulus correlation used in the original method proposed by the previous authors, didn't give a good prediction for the study area chosen in this study, another correlation has been chosen, which is depends on porosity value and velocity ratio gave more acceptable results.
- 5- The model in the tight zones of the reservoir showed similar behavior in all of these zones along the open-hole section. While, in clay-rich zones such as marls or shales, the model gave erroneous results due to raw sonic and porosity logs are highly affected by the washout of these intervals.
- 6- The model is a highly predictive tool in the oil and water zones of high porosity greater than 0.1 p.u., the model oil curve is matching sonic transit time along the oil zone with a clear separation between oil and water curves, and that separation increases in the good reservoir characteristics zones and less in poor characteristics zones. Hence, Separation increases with increasing characteristics.
- 7- The method applicability in the study area is good after modification regarding the properties of rock and fluids.
- 8- As suggested by original authors it can be used as an assistant tool independent from conventional methods that rely on resistivity tools, in exploration wells. And

also it can be used in time-lapse monitoring of the reservoir, after water flooding to monitor the breakthrough from sonic log only. Thus it is a low cost good predictive tool.

## Nomenclatures

$\Delta t_p$ :	compressional transit time, $\mu\text{sec}/\text{ft}$ .
$\Delta t_s$ :	shear transit time, $\mu\text{sec}/\text{ft}$ .
$B_o$ :	Oil FVF, BBL/STB.
$G$ :	Rock shear modulus, GPa.
$K_b$ :	Rock bulk modulus, GPa.
$K_{fl}$ :	Fluid bulk modulus, GPa.
$K_{fr}$ :	Dry frame bulk modulus, GPa.
$K_{ma}$ :	Matrix bulk modulus, GPa.
$N_{phi}$ :	Neutron porosity, fraction.
$P$ :	formation pressure, MPa,
$R_G$ :	gas oil ratio, L/L.
$S$ :	Salinity, (ppm/1000000).
$T$ :	Formation Temperature, Celsius.
$V_{Brine}$ :	sound velocity in Brine, ft/sec.
$V_{oil}$ :	sound velocity in oil, ft/sec.
$V_p$ :	Compressional velocity, ft / $\mu\text{sec}$ .
$V_s$ :	Shear velocity, ft / $\mu\text{sec}$ .
$V_w$ :	sound velocity in fresh water, ft/sec.
$\gamma_{gas}$ :	Gas gravity, unitless.
$\rho_o$ :	oil density @Reservoir Cond., gm/cc.
$\rho_b$ :	rock bulk modulus, gm/cc.
$\rho_{Brine}$ :	Brine density @Reservoir Cond., gm/cc.
$\rho_{oil}$ :	oil density @surface, gm/cc.
$\rho_{p\&T}$ :	oil density corrected for P&T, gm/cc.
$\rho_p$ :	oil density corrected for pressure surface, gm/cc.
$\rho_w$ :	fresh water density @Reservoir Cond., gm/cc.
$\Phi_T$ :	$\Phi_T$ : total porosity, fraction.

## References

- [1] [R. Ramamoorthy and W. F. Murphy, "Fluid identification through dynamic modulus decomposition in carbonate reservoirs," paper Q in 39th Annual Logging Symposium Transactions: Society of Professional Well Log Analysts, 1998.](#)
- [2] [W.W. Souder, "Using Sonic Logs to Predict Fluid Type," Society of Petrophysicists and Well-Log Analysts, 1 Sep. 2002.](#)
- [3] [E. Fjær, R. M. Holt, A. M. Raaen, and R. Risnes, "Chapter 5 Elastic wave propagation in rocks," in Petroleum Related Rock Mechanics, vol. 53, Elsevier, 2008, pp. 175–218.](#)
- [4] [J. W. Minear and C. R. Fletcher, "Full-Wave Acoustic Logging," SPWLA 24th Annual Logging Symposium, Society of Petrophysicists and Well-Log Analysts, 1983.](#)
- [5] [M. R. Wyllie, A. R. Gregory, and L. W. Gardner, "Elastic Wave Velocities in Heterogeneous and Porous Media," Geophysics, vol. 21, no. 1, Jan. 1956.](#)
- [6] [O. Serra, The acquisition of logging data, Elsevier, 1985.](#)
- [7] [A. M. Aqrabi, J. C. Guff, A. D. Horbury, and F. N. Sadooni, Petroleum Geology of Iraq, vol. 1, 1 vols. Aberystwyth, UK: Scientific Press Ltd., 2010.](#)
- [8] [S. Z. Jassim and T. Buday, "Units of Stable Shelf," in Geology of Iraq, 1st ed., Brno, Czech Republic: Dolin, 2006, pp. 57–70.](#)

- [9] M. Embong, M. Higashi, H. H. Abu Bakar, K. A. Zamri, F. H. M Ali, S. Moriya, S. B. M Said, and A. T. Patrick Panting, "Petroleum Geoscience Conference & Exhibition2012," in Reservoir Characterisation of Mishrif Formation of Garraf field, Iraq, using 3D seismic and AI Inversion, 2012.
- [10] [Z. Wang, W.K. Hirsche, and G. Sedgwick, "Seismic velocities in carbonate rocks," \*Journal of Canadian Petroleum Technology\*, pp. vol. 30, No.2, pp. 112 – 122, March-April, 1991.](#)
- [11] [J.H. Schön, \*Physical properties of rocks\*, 2nd ed., vol. 65. Amsterdam, Netherlands: Elsevier, 2015.](#)
- [12] [D. V. Ellis and J. M. Singer, \*Well logging for earth scientists\*, 2nd ed. \*Springer\*, 2007.](#)
- [13] [D. Han and M. Batzle, "Constrained and Simplified Gassmann's Equations.," \*Society of Exploration Geophysicists\*, pp. 1837–1841, 2002](#)
- [14] [G. Mavko, J. Dvorkin, and T. Mukerji, \*The rock physics handbook: Tools for Seismic Analysis of Porous Media\*. Cambridge, UK: \*Cambridge University Press\*, 2009.](#)
- [15] [J. E. White, \*Underground Sound: Application of Seismic Waves\*, 1st ed. Amsterdam: \*Elsevier\*, 1983.](#)
- [16] N. Al-Khateb, "A look into Gassmann's Equation," in *Geoconvention2013*, Calgary, Canada, 2013.
- [17] A. E. H. LOVE, *A Treatise on the Mathematical Theory of Elasticity*, 4th ed. NY: Dover Publications, pp. 103–294, 1944.
- [18] [M. Batzle and Z. Wang, "Seismic properties of pore fluids," \*Geophysics\* vol. 57, pp. 1396–1408, 1992.](#)
- [19] [Z. Wang, M.L. Batzle, and A. Nur, 1990, "Effect of different pore fluids on seismic velocities in rocks," \*Can. J. Expl. Geophys.\*, vol. 26, pp. 104-112. 1990.](#)
- [20] [V. Saxena, "Fresh Sonic Interpretation in Limestone Through Modulus Decomposition," \*Society of Petroleum Engineers\*, New Delhi, India, 1998.](#)
- [21] [G.R. Pickett, "Acoustic Character Logs and Their Applications in Formation Evaluation," \*Society of Petroleum Engineers\*, USA, 1 Jun. 1963.](#)



Appendix A: Garraf oilfield Lithological Column, after Ref [7]

		Age		Formation	Generalized Lithology	Estimated Thickness (m)	Reservoir		
<b>Cenozoic</b>	<b>Tertiary</b>	Neogene	M. Miocene	U. Fars		628 - 661			
				L. Fars		177 - 200			
		Paleogene	M. Oligocene	Bajawan		76 - 84			
				Baba					
				Tarjil					
			E. Oligocene	Palani		39 - 44			
		E. Eocene - Paleocene	L.M. Eocene	Dammam		80 - 92			
				Rus / UeR		297 - 303			
				Aaliji		302 - 309			
		<b>Mesozoic</b>	<b>Cretaceous</b>	L. Cretaceous	U. Campanian - Maastrichtian	Shiranish		142 - 144	
						Hartha		144 - 158	
					U. Turonian - L. Campanian	Sadi		166 - 178	
						Tanuma		48 - 50	
						Khasib		46 - 54	
M. Cretaceous	Cenomanian - Turonian			Mishrif		288 - 301	●		
				Rumaila		40 - 41			
	Albian			Ahmadi		12			
				Mauddud		202 - 209			
				Nahr Umr		131 - 140			
E. Cretaceous	Barriasian - Aptian			Shuaiba		66 - 73			
				Zubair		436 - 446	●		
				Ratawi		160 - 167	●		
				Yamama		269 - 279	●		
				Sulaiy		230 - 260			
<b>Jurassic</b>	L. Jurassic			Oxfordian - Tithonian	Gotnia		260 - 290		
					Najma		421	□ ?	
	M. Jurassic			Bajocian - Callovian	Sargelu		367		
					Alan/Mus / Adaiyah		272	□ ?	
	E. Jurassic			Liassic	Butmah		295	□ ?	
Trias - sic	Late	Kurra Chine							

**Appendix B: Fluid Elastic Properties**

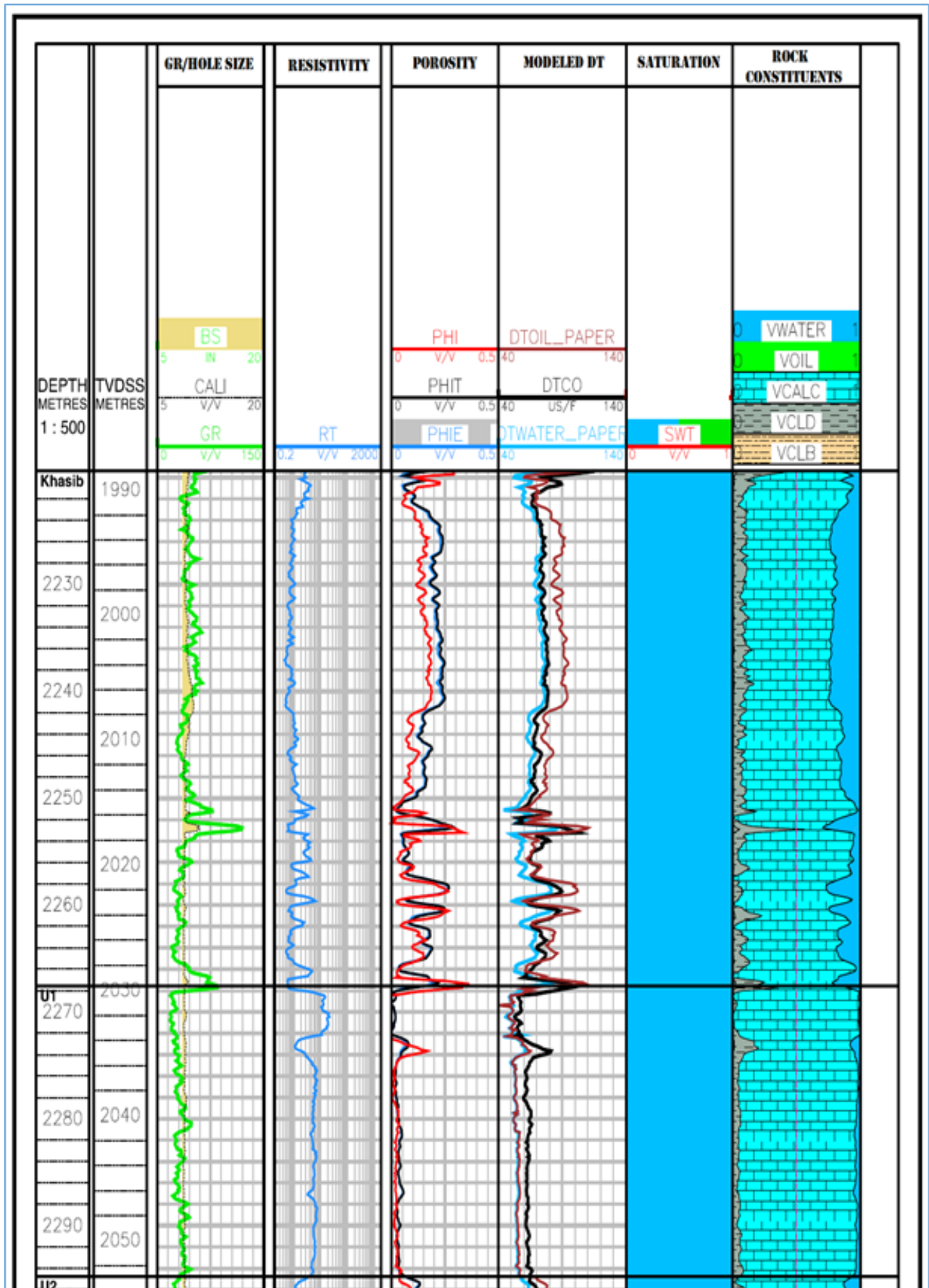
Table 2. Oil properties

	Zone	M1	L1.1	L1.2
Dead Oil	API@15 °C	24.06	24.35	25.37
	P (MPa)	20.898	23.814	23.263
	T (°C)	79.7	77.8	79
	$\rho_o$ (g/cc)	0.9096	0.9079	0.902
	$\rho_o$ @P (g/cc)	0.9202	0.92	0.914
	$\rho_o$ @T (g/cc)	0.8724	0.8738	0.8671
	$V_o$ ft/s	4598.53	4685.94	4648.7
	$K_o$ (GPa)	1.71385	1.78244	1.7408
Live Oil	$\gamma_g$	0.938	0.943	0.946
	RG (L/L)	119	143.13	143.37
	$B_o$ (RB/STB)	1.3914	1.4645	1.469
	$\rho'_o$ (g/cc)	0.7842	0.712193	0.623093
	$K_i$ (Gpa)	1.5406	1.4528	1.251

Table 3. Water properties

Studied Well								
Brine								
Zone	T (°C)	P (MPa)	Ppm/10 <sup>-6</sup>	$\rho_w$ (g/cc)	$\rho_{br}$ @P (gm/cc)	$V_w$ (m/s)	$V_{br}$ (ft/s)	$K_w$ (Gpa)
Khasib	76	20.753	0.0998	1	1.0688	1598.65	5528.5	3.0353
U1	77.3	20.864	0.1	1	1.0688	1598.77	5528.3	3.0351
U2	78	21.057	0.1	1	1.0688	1598.8	5527.8	3.0346
Marl	77.8	21.512	0.11	1	1.0689	1598.8	5556.8	3.0665
L2	79.4	23.539	0.114	1	1.069	1598.82	5566.3	3.0771

**Appendix C:** Well log interpretation along with the proposed model curves



## إستخدام الخواص المرنة للصخور كأداة تنبؤية لنوع المائع في مسامات الصخور الكاربونية

### الخلاصة

إنَّ الهدف من هذه الدراسة، هو لفحص تطبيق طريقة تنبؤية لنوع المائع المسامي المنشورة من قبل رامامورثي ومورفي، لإحدى تكوينات الشرق الأوسط الكاربونية. وكذلك تضمنت إستخدام نتائج ساوذر الذي إستخدم مبدأ رامامورثي-مورفي في توقع نوع المائع المسامي في صخور بحر الشمال الطباشيرية. ولقد تناولت هذه الدراسة تكوين المشرف في حقل الغراف الواقع في جنوب العراق، من خلال بئر شبه عمودي محفور إلى تكوين المشرف. وقد إستخدمت بيانات المجسات في التكوين المفتوح وخصوصا المجس الصوتي ذو الطورين (القصي والإنضغاطي) وبيانات الوصف الجيولوجية وبيانات الفحوصات المختبرية للسوائل المكمئية (PVT) لغرض إشتقاق الخواص المرنة لهذه الموائع بإستخدام معادلات باتزل ووانغ. تم إستخدام مجس الكثافة و قياسات سرعة القص لإشتقاق معامل القص للصخرة لكل (0.1254 متر) على طول التجويف. أما معامل الإنضغاطية للصخرة الجافة فقد تم إشتقاقه من معادلة ساكسينا، بدلا عن المعادلات المتبعة في الدراستين السابقتين بسبب الحاجة إلى دراسة تفصيلية للباب لغرض معرفة نوع المسامية. تم إستخدام معادلة غاسمان لحساب معامل الإنضغاطية الكلي للصخرة بظروف تشبع مختلفة (100% ماء) و(100% نפט)، وتم ربطها بمعادلات لوف لإشتقاق قيمة زمن الإنتقال الأنضغاطي (مقلوب السرعة) بإستخدام المعاملات الناتجة من معادلة غاسمان. بعد ذلك تم دمج المنحنيات الناتجة مع منحنى المجس الصوتي الإنضغاطي وكذلك مع تفسير التجويف المفتوح من مسامية وتشبع وصخارية. وقد بينت الدراسة إن الطريقة هي دليل جيد على نوع المائع المسامي، وخصوصا في مناطق المسامية الجيدة. وبعكسه في المناطق القليلة النفاذية فهي غير مفيدة. وقد كانت النتائج متوافقة بشكل ممتاز مع التفسيرات الأخرى، فقد أعطت عمق تماس النفط-الماء بشكل ممتاز ومثابه للعمق الناتج من منحنى التشبع الناتج من المقاومة النوعية العميقة، بهامش خطأ أقل من (0.03%).